



Flexible and freestanding electrode based on polypyrrole/graphene/bacterial cellulose paper for supercapacitor



Lina Ma^a, Rong Liu^a, Haijun Niu^b, Min Zhao^a, Yudong Huang^{a,*}

^a MIIT Key Laboratory of Critical Materials Technology for New Energy Conversion and Storage, State Key Laboratory of Urban Water Resource and Environment, School of Chemistry and Chemical Engineering, Harbin Institute of Technology, Harbin 150001, PR China

^b Key Laboratory of Functional Inorganic Material Chemistry, Ministry of Education, Department of Macromolecular Materials and Engineering, School of Chemical and Chemical Engineering, Heilongjiang University, Harbin 150080, PR China

ARTICLE INFO

Article history:

Received 7 August 2016
Received in revised form
26 October 2016
Accepted 28 October 2016
Available online 31 October 2016

Keywords:

Bacterial cellulose
Polypyrrole
Graphene
Flexible electrode
Supercapacitor

ABSTRACT

A simple and low-cost approach toward flexible and freestanding electrode is developed. The method involves coating the polypyrrole (PPY) encapsulated graphene (RGO) composites on bacterial cellulose, from which large mass loading of 8.93 mg cm⁻² is obtained. Benefiting from the well structural features, the flexible PPY/RGO/BC paper can be directly acted as supercapacitor electrode without metallic current collectors, binder and additives, and achieves a high areal capacitance (2100 mF cm⁻² at 2 mA cm⁻²), good rate performance (1570 mF cm⁻² retention at 50 mA cm⁻²) and high flexibility (suitable for arbitrary angles, even 180°). Moreover, the assembled symmetric supercapacitor delivers as high as 790 mF cm⁻² of areal capacitance and 0.11 mWh cm⁻² of energy density. Therefore, this strategy provides a facile method for design of flexible supercapacitor electrodes with high areal capacitance.

© 2016 Elsevier Ltd. All rights reserved.

1. Introduction

Flexible energy storage devices have attracted tremendous attention in recent years, the potential applications of which ranging from wearable electronics, stretchable electronics, collapsible displays to on-body sensors [1–5]. Among various types of energy storage devices, supercapacitors are widely recognized as an important class due to high power density, fast dynamic response, moderate energy density, good operational safety, and long life cycle [6–9]. However, restrained by the lack of flexibility and lightweight of conventional supercapacitors, one of the key challenges is to fabricate flexible and freestanding electrodes with high capacitance and good mechanical properties [10].

To date, considerable efforts have focused mainly on improving the gravimetric capacitance of the flexible electrodes, but for wearable and portable electronics, areal and volumetric performance are at a premium [11]. In general, supercapacitors can be classified into two categories based on charge-storage mechanism, namely the electrochemical double-layer capacitors (EDLCs) and pseudo-capacitors (PDCs). Carbon based freestanding film

including RGO paper and carbon nanotubes paper are very popular to be employed for flexible electrodes in EDLCs due to the high conductive property and large surface area, and the charges are electro-statically stored by reversible ion adsorption at the electrode/electrolyte interface [12–14]. Despite these carbon based flexible paper has shown long cycle life and good gravimetric capacitance, the areal capacitance (<100 mF cm⁻²) is rather low due to the small mass loading (<1 mg cm⁻²) [15]. PDCs, based on fast reversible faradic reactions at the surface of electroactive materials, using conducting polymers or metal oxides as active materials provide them with several times higher specific capacitance than the non-faradic EDLCs. PPY, as a kind of traditional conducting polymer, is particularly promising pseudocapacitive electrode material for supercapacitors owing to its high energy storage capacity, high electrical conductivity in doped states, ease of low cost synthesis and low environmental impact [16–18]. Nevertheless, poor cycling stability induced by large volumetric swelling and shrinking during charge/discharge and weak flexibility of PPY limit its use in flexible supercapacitors. A number of methods have been demonstrated to overcome these drawbacks by coupling PPY onto flexible supporting substrates such as office paper, RGO paper, and carbon nanotube film. Therefore, directly electro-polymerization or chemical polymerization PPY onto carbon-based electrical

* Corresponding author.

E-mail address: yduang.hit1@aliyun.com (Y. Huang).

conductivity substrates is the main approach. However, the mass loading of these electrodes is generally still very low, resulting in the low areal capacitance, despite that they have obtained high electrical conductivity, good gravimetric performance and rate capability [19].

As has been described recently, porous textiles are also used as alternative substrate. In comparison to printing paper and carbon conductive paper, they can provide three-dimensional (3D) porous network structure, and therefore enable high mass loading. As an interesting ecofriendly biomaterial cellulose, BC is produced by fermentation of bacteria (*Acetobacter xylinum*, *E. coli*, etc.). With so many unique properties such as specific ultrafine network structure, good mechanical strength and high water holding capability, BC could be designed and applied in supporting substrates. Furthermore, while great efforts have been devoted to develop high capacitive devices, relatively fewer attentions have been paid to its mechanical properties. Designing efficient, low-cost flexible electrode that can achieve both good electrochemical properties and high mechanical integrity upon bending or folding, tensile strength and lightweight property is highly required [15]. In this point of view, BC membrane can strongly bind with PPY and carbon materials due to the many hydroxyl groups, meanwhile, the stretchable and compressible properties of these structures can be helpful for mechanical properties of flexible electrode.

Herein, we demonstrate a simple and low-cost “polymerization and vacuum-filtering” method to fabricate the PPY/RGO/BC flexible electrode. The as-constructed flexible electrode exhibits good electrochemical performance and mechanical properties. The as-fabricated paper with high mass-loading ($\sim 8.93 \text{ mg cm}^{-2}$) shows a high areal capacitance of 2100 mF cm^{-2} , good rate performance (75% retention at 50 mA cm^{-2}) and good cycling stability with $\sim 64.7\%$ of its initial capacitance after 5000 cycles. By direct coupling of two paper electrodes, symmetric supercapacitor can offer large areal capacitance (790 mF cm^{-2}), high energy density of 0.11 mWh cm^{-2} and power density of 15 mW cm^{-2} . Therefore, this strategy opens up new opportunities for development of high performance flexible energy-storage devices.

2. Experimental

2.1. Preparation of PPY/RGO

RGO suspension (0.5 mg ml^{-1}) was obtained by a modified Hummers method and referred to the previous papers [15,20]. PPY/RGO composite was prepared by the in situ polymerization of pyrrole monomer and RGO aqueous dispersion in the presence of FeCl_3 as an oxidant and $\text{C}_7\text{H}_8\text{O}_3\text{S} \cdot \text{H}_2\text{O}$ (*P-TSA*) as a dopant. Typically, 0.2 ml pyrrole monomer and 532 mg *P-TSA* were added into the 50 ml RGO suspension with strong mechanical stirring for 1 h in an ice-water bath. 778 mg ferric chloride was dissolved in 30 ml deionized water and added dropwise into the pyrrole/RGO suspension with constant stirring for 1 h at $0\text{--}5^\circ\text{C}$ to obtain PPY_1/RGO suspension. The other samples of PPY_2/RGO , PPY_4/RGO , PPY_6/RGO and PPY_8/RGO were conducted by prolonging the polymerization times for 2, 4, 6 and 8 h.

2.2. Preparation of PPY/RGO/BC hybrid membrane

To obtain a uniform BC suspension, BC pellicle (Hainan Yide Foods Co. Ltd.) was first neutralized with deionized water, and then cut into small slices, followed pulped with a mechanical homogenizer at the speed of $10,000 \text{ r min}^{-1}$. The collected suspension (200 ml , 0.7 mg ml^{-1}) was drained on a nitro cellulose filter membrane (porous size of $0.22 \mu\text{m}$) to get a uniform BC paper by vacuum filtration. Subsequently, the as-prepared PPY_x/RGO ($x = 1,$

2, 4, 6 and 8) suspension was poured onto the BC paper to obtain a filter cake and dried at 60°C overnight, and then peeled off to get the freestanding $\text{PPY}_x/\text{RGO}/\text{BC}$ film. The active materials of PPY_1/RGO , PPY_2/RGO , PPY_4/RGO , PPY_6/RGO and PPY_8/RGO were $5.78, 6.74, 7.81, 8.93$ and 9.14 mg cm^{-2} , respectively.

2.3. Characterization and electrochemical measurements

The morphology and microstructure of the samples were characterized through scanning electron microscope (SEM, Hitachi S-4800) and transmission electron microscope (TEM, JEM-2100 F). The functional group distribution was investigated by Fourier transform infrared spectroscopy analyzer (FT-IR, PerkinElmer Spectrum 100 Model) and X-ray diffraction (XRD, Rigaku 2500) equipped with $\text{Cu K}\alpha$ radiation ($\lambda = 1.5406 \text{ \AA}$). X-ray photoelectron spectroscopy (XPS, VG ESCALABMK II) was carried out to investigate the surface elemental compositions. Electrochemical studies were performed with a CHI660E electrochemical workstation. The single electrode was tested in a three-electrode system in 1 M NaNO_3 aqueous solution with active carbon and a saturated calomel electrode (SCE) as the counter electrode and reference electrode, respectively. Symmetric supercapacitor was measured in two electrode configuration using both flexible $\text{PPY}/\text{RGO}/\text{BC}$ hybrid paper as electrodes, which separated with diaphragm.

3. Results and discussion

Synthetic procedure of $\text{PPY}/\text{RGO}/\text{BC}$ is presented in Fig. 1. The PPY/RGO was first prepared through in situ polymerization using pyrrole and *P-TSA* as the monomer and dopant, respectively. The grown PPY thickness is roughly tunable with polymerization time. Then, the PPY/RGO composite was poured onto the prepared BC paper, black active materials spontaneously dispersed into the 3D porous network to form a hybrid paper with large mass loading. The flexible paper can be directly acted as supercapacitor electrode without metallic current collectors, binder and additives.

Fig. 2 presents the typical morphology and microstructure of BC, RGO, PPY_6/RGO and $\text{PPY}_6/\text{RGO}/\text{BC}$ composites. The BC pellicle (Fig. 2a) shows a water rich morphology due to a large number of hydrophilic groups along its network. The SEM image illustrates that the BC consists of continuous nanofibers to form a porous and interconnected network structure (Fig. 2b). Further characterization by TEM demonstrates that the diameter of BC nanofibers is $20\text{--}60 \text{ nm}$ (Fig. 2c). The BC with porous network serves as a substrate to provide a large surface area for active materials, while high hydrophilicity of BC can effectively enable the contact between active materials and aqueous electrolytes and reduce the diffusion distance of electrolyte ions during the charge/discharge process. The SEM image of RGO in Fig. 2d reveals a wrinkled and crumpled features, which could be identified in Fig. 2e. Fig. 2f shows the SEM image of $\text{PPY}_6/\text{RGO}/\text{BC}$ paper, it is observed that highly uniform PPY grown on the surface of RGO nanosheets, and then assembles into BC to form the freestanding electrode. It is worth noting that $\text{PPY}_6/\text{RGO}/\text{BC}$ paper retains the porous nanoarchitectures, which can be help for electrolyte transport and active-site accessibility. Moreover, such freestanding paper (0.28 mm thickness) exhibits high flexibility and can be bended for a large angle (Fig. 2i), which enables the practical applications on flexible and lightweight energy storage devices. Further observation from the TEM of PPY_6/RGO (Fig. 2g) indicates that the RGO is distinctly enwrapped with gauze-like PPY. Moreover, the high resolution TEM image exhibits direct evidence that randomly orientated PPY is assembled along the RGO nanosheets (Fig. 2h). The RGO is uniformly sandwiched between PPY, which forms two potential benefits for flexible electrode. First, this architecture could act as a buffering layer to prevent the severe

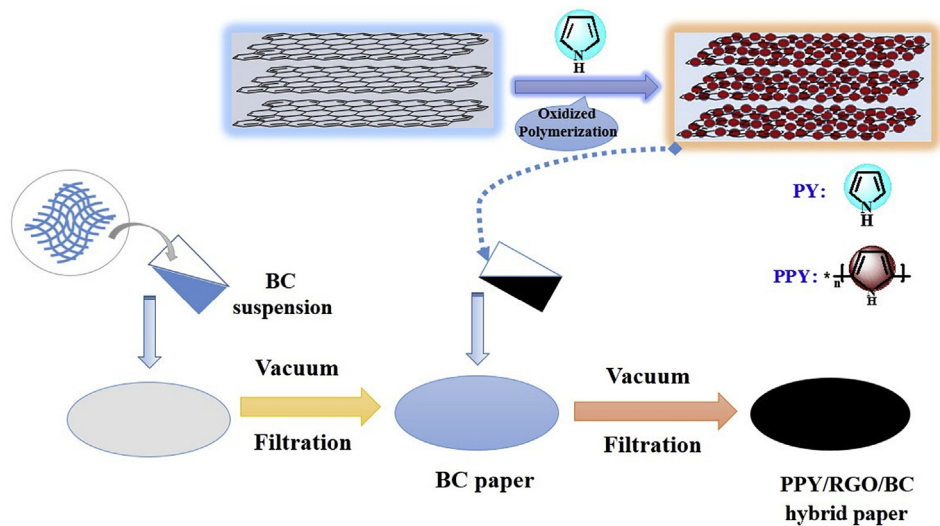


Fig. 1. Schematic illustration of the fabrication process of PPY/RGO/BC paper electrode.

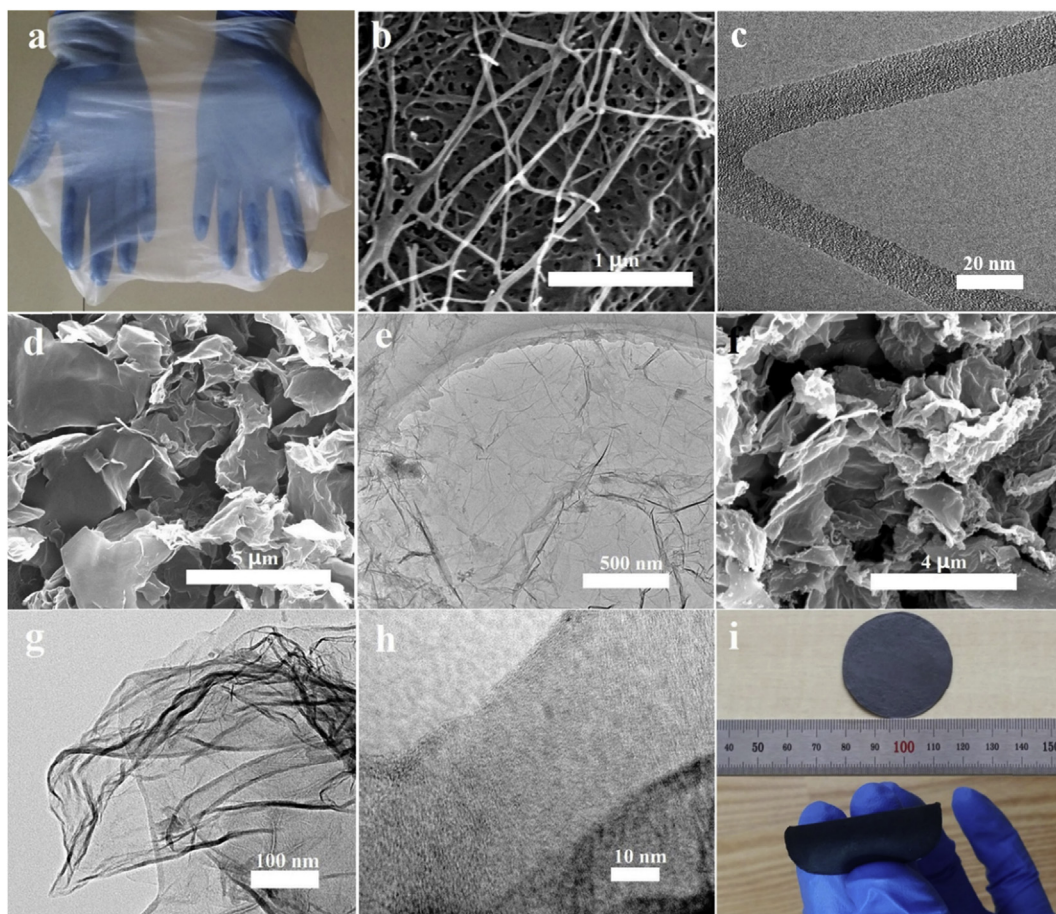


Fig. 2. (a) Photograph of BC slice. (b,c) SEM and TEM images of the BC. (d,e) SEM and TEM images of RGO. (f) SEM image of PPY₆/RGO/BC. (g,h) High-resolution TEM images of PPY₆/RGO. (i) Photograph of PPY₆/RGO/BC paper.

swelling and shrinking of PPY during the charge/discharge process and maintain electrochemical stability. Second, it could serve as a conductive networks ensuring fast electron transportation throughout the electrode.

FTIR spectroscopy was performed to characterize the PPY and

PPY/RGO structure, as shown in Fig. 3a. There is no obvious adsorption peak of RGO, suggesting the functional groups have been essentially removed from the oxide graphene. For PPY, the main characteristic peaks located at 3416, 1557, and 1458 cm^{-1} are related to the antisymmetric and symmetric pyrrole ring vibration,

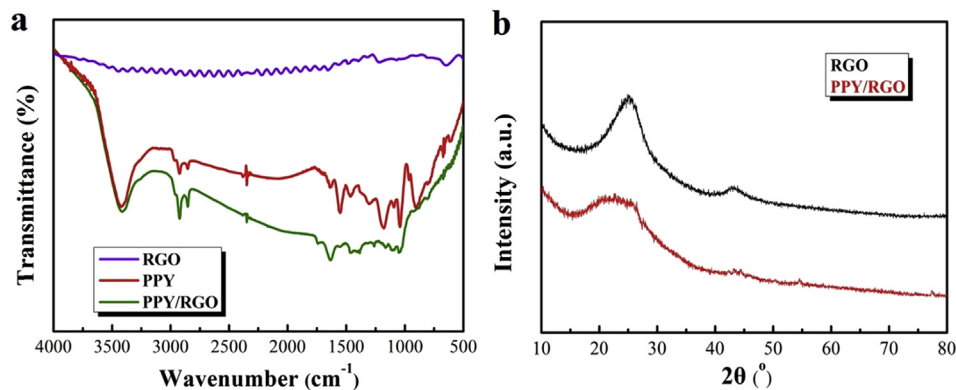


Fig. 3. (a) FTIR spectra of RGO, PPY and PPY/RGO. (b) XRD patterns of RGO and PPY/RGO.

respectively [21]. While the bands at 1294 and 1036 cm^{-1} are considered as the C–N stretching and C–H bond in-plane vibration of the PPY. Moreover, the peaks at 2923 and 2845 cm^{-1} are attributed to the asymmetric stretching and symmetric vibrations of CH_2 [22]. Meanwhile, the peak at 1186 and 1639 cm^{-1} correspond to stretching of the sulfonic group from *p*-TSA and the C=C backbone stretching [23]. All results indicate the successful formation of PPY. While for the PPY/RGO composite, the typical peaks attributed to PPY still remain, but they have a red-shift in comparison with that of PPY, implying that the RGO is incorporated into the PPY successfully [24]. Additionally, XRD analysis (Fig. 3b) identify the two characteristic broad peaks of RGO at 25.2 and 43.0 , and after polymerization, the PPY/RGO composite also shows the amorphous structure.

Furthermore, XPS was further performed to analyze the chemical states, protonation and doping level of PPY/RGO. The typical characteristic peaks in the survey spectra (Fig. 4a) suggest that the RGO is indeed coated with PPY. Moreover, the high resolution spectrum of N1s spectrum is fitted by three decomposed peaks (Fig. 4b), namely 399.1 eV (benzenoid amine, $-\text{NH}-$), 401.2 eV (protonated benzenoid amine, $-\text{N}^+\text{H}-$), and 402.2 eV (protonated quinonoid imine, $=\text{N}^+-$), respectively. The doping level can be estimated by the positively charged nitrogen (N^+) ratios [24]. Hence, the higher doping level can promote the electronic conductivity of PPY, which could be help for the rate performance on this flexible supercapacitor electrode.

To learn the effect of wettability of the PPY₆/RGO/BC hybrid paper, the dynamic water contact angle measurement was performed. Different wetting time is presented as shown in Fig. 5, the hybrid paper is highly hydrophilic with the initial contact angle of

55° and the droplet is completely absorbed within 4 s. The positive result mainly attributes to the porous structure of PPY₆/RGO/BC paper and large amount of hydrophilic groups of BC [17], which provide a superabsorbent and facilitate ion transport within the electrode.

In order to demonstrate the advantages of large mass amount, flexible and freestanding PPY/RGO/BC paper as a supercapacitor electrode, electrochemical measurements were carried out in a three-electrode system in a 1.0 M NaNO_3 electrolyte. Fig. 6a compares the cyclic voltammetry (CV) curves of PPY/RGO/BC electrodes with different polymerization time in the potential window of -0.4 – 0.6 V collected at 10 mV s^{-1} . All CV curves show symmetric and nearly rectangular shapes without obvious redox peaks, demonstrating highly consecutive and reversible Faradaic reaction over the entire CV process, which is also consistent with other literature of PPY [25,26]. As expected, current density and integrated CV area of PPY₆/RGO/BC are significantly higher than other electrodes, indicating that the loading amount plays a central role in areal capacitance. Fig. 6b shows CV curves of the PPY₆/RGO/BC flexible electrode at different scan rates of 1 – 50 mV s^{-1} . Notably, the response current increases with the increase of scan rate, reflecting that the PPY₆/RGO/BC paper has a good capacitive behavior and high rate capability, which can be attributed to the fast electron transfer and rapid diffusion of electrolyte ions through the porous network. Fig. 6c displays the galvanostatic charge-discharge (GCD) curves at different current densities ranging from 2 to 50 mA cm^{-2} . The charge-discharge curves are nearly symmetric triangular with a slight curvature, and small iR drop is observed at a high current density of 10 mA cm^{-2} .

Considering the practical application, areal specific capacitance

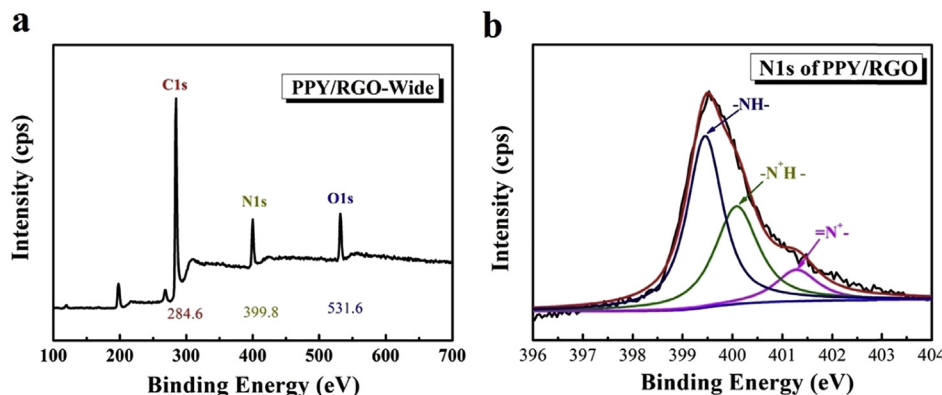


Fig. 4. (a) XPS survey spectra of PPY/RGO. (b) High-resolution XPS spectra of the deconvoluted N1s.

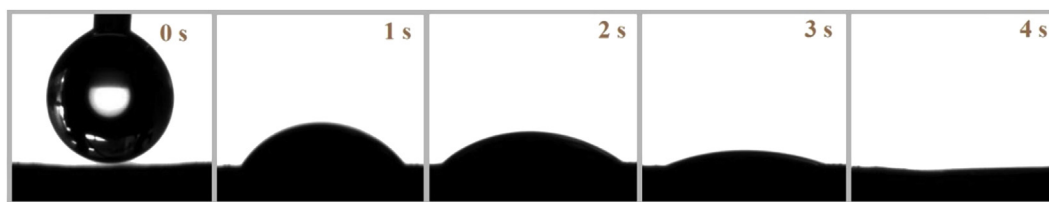


Fig. 5. Dynamic water contact angle measurement for the PPY₆/RGO/BC.

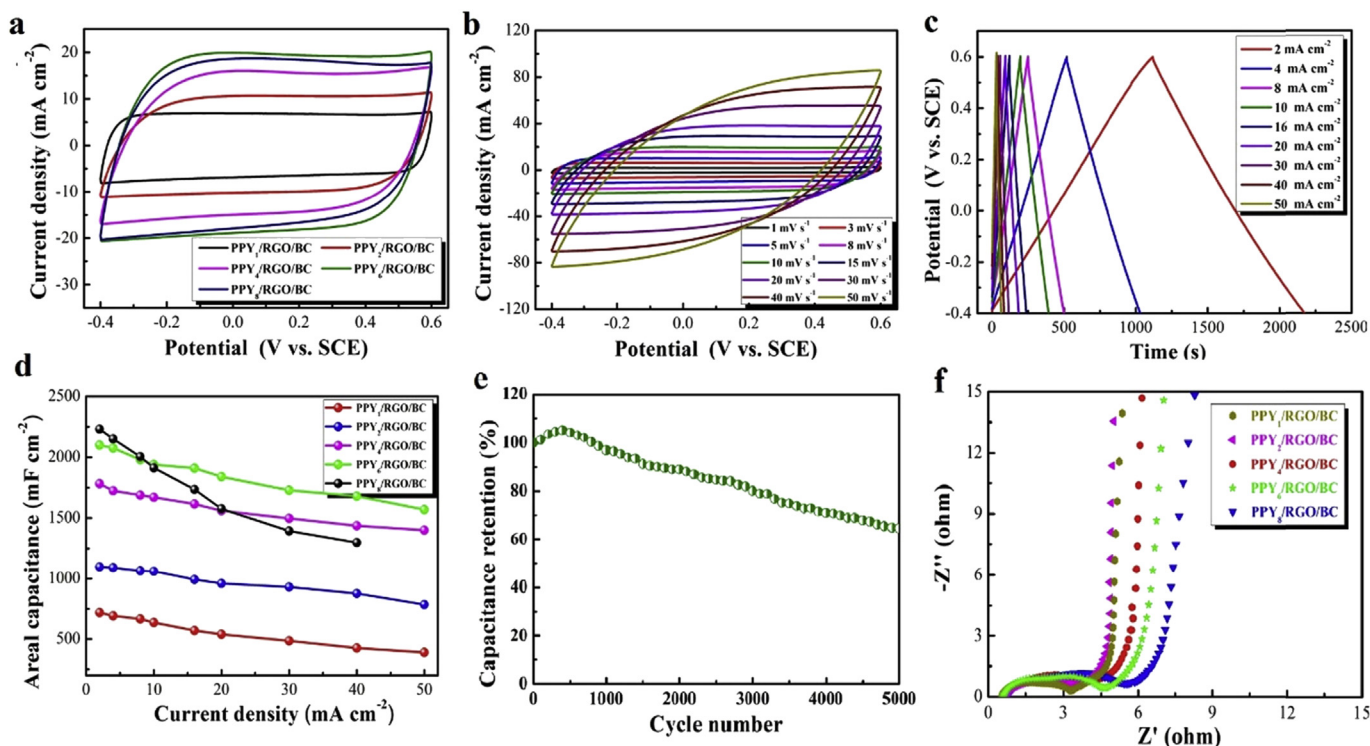


Fig. 6. Electrochemical performance of the PPY/RGO/BC electrodes. (a) Comparison of CV plots at 10 mV s^{-1} (b) CV curves at different scan rates. (c) GCD curves at different current densities. (d) Areal capacitance at different current densities. (e) Cycle stability of PPY₆/RGO/BC electrode at the current density of 20 mA cm^{-2} at room temperature. (f) Nyquist plots.

is considered as a more important factor to evaluate film electrodes for flexible supercapacitors, which can be calculated from charge and discharge test and the values are plotted as a function of current densities in Fig. 6d. The areal capacitance of the paper increases with prolonging the polymerization time from 1 to 6 h and reaches the maximum value due to the increase of the incorporating pseudocapacitance. However, the areal capacitance decreases at the reaction time of 8 h. This result is mostly caused by the increase thickness of PPY on RGO, which blocks the diffusion of ions into the interior of the materials. The PPY₆/RGO/BC paper achieves the highest areal capacitance of 2100 mF cm^{-2} (235.2 F g^{-1}) at a current density of 2 mA cm^{-2} , and still retains 1570 mF cm^{-2} (175.8 F g^{-1}) at a current density of 50 mA cm^{-2} . Hence, we employ the PPY₆/RGO/BC as the flexible electrode of our symmetry supercapacitor. In addition, the PPY₆/RGO/BC electrode shows good cyclic stability of 64.7% capacitance retention after 5000 cycles at 20 mA cm^{-2} (Fig. 6e). As known that the poor cycle life is an important drawback for PPY electrode material. PPY backbones may suffers from swelling/shrinking associated with the doping/de-doping of ions during charge/discharge process, resulting in irreversible phase change, especially for large electroactive material mass [27–29]. Herein, the electrochemical stability of

PPY₆/RGO/BC electrode was examined under continuous charge–discharge test at 20 mA cm^{-2} for 5000 cycles. The flexible electrode with large mass also shows good cyclic stability of 97.1% capacitance retention after 1000 cycles, and 64.7% retention can be obtained after 5000 cycles, and the performance can reach general level of recent conductive polymer flexible electrode. (Fig. 6e). This could be attributed to the “skeleton/skin” structure of PPY/RGO, which can inhibit the volumetric alternation of PPY to some extent.

The electrochemical performances of various hybrid electrodes were further investigated by electrical impedance spectroscopy (EIS), and the Nyquist plots are shown in Fig. 6f. All plots feature a semicircle and a linear part in the high- and low-frequency regions, which are considered to be related to an interfacial charge-transfer resistance and capacitive behavior. The impedance profiles exhibit the most vertical line, indicating an ideal capacitive performance. It is observed that the radius of the semicircle slightly increases with the reaction time, revealing an increasing of interfacial resistance and decreasing of the conductivity of the PPY/RGO/BC, which is mainly ascribed to the low-conductive PPY grown onto the surface of high-conductive RGO.

The good electrochemical performance can be attributed to the following benefits: First, the BC not only enable the high mass

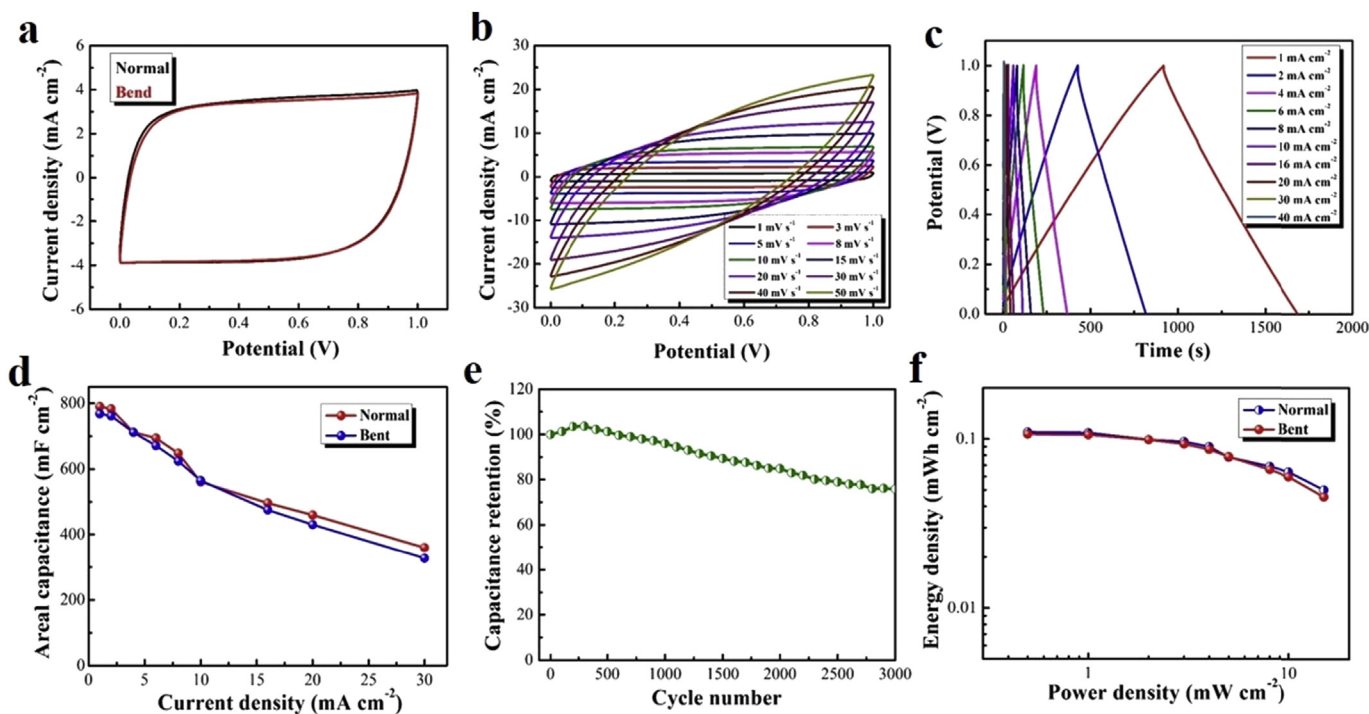


Fig. 7. Electrochemical performance of the PPY₆/RGO/BC symmetrical supercapacitor. (a) CV curves under bending and flat condition at 5 mV s⁻¹ (b) CV curves at different scan rates. (c) GCD curves under different current densities. (d) Areal capacitance versus different current densities at normal and bending condition. (e) Cycling performance at a current density of 10 mA cm⁻². (f) Ragone plot.

Table 1
Literature on flexible electrodes for supercapacitor application.

Flexible materials	Mass (mg cm ⁻²)	Capacitance (mF cm ⁻²)	Capacitance (F g ⁻¹)	Cycling capability (cycles)	Ref.
PPy/carbon cloth electrode		136.99	114.08	85% after 10,000	[16]
PPY hydrogels	20	6400		93% after 2000	[27]
GWF/PANI supercapacitor		23	771	100% after 2000	[30]
PANI/Au/paper electrode	14	800	560		[31]
PPy/gold supercapacitor		1.8	270	78% after 900	[32]
PPY/rGO	2.7	440 (0.5 A g ⁻¹)	163	78% after 1000	[33]
rGO/PPY NT		807 (1 mA cm ⁻²)		78% after 1000	[34]
GN/PPY	0.25	37		91% after 5000	[35]
PPY printing paper	3.54	420 (1 mA cm ⁻²)		75.6% after 10,000	[36]
PPY/RGO/BC electrode	8.93	2100 (2 mA cm ⁻²)	235.2	~64.7% after 5000	Our work
Symmetric supercapacitor		790 (1 mA cm ⁻²)		75.8% after 3000	

loading, but also shorten the ions diffusion distance and maximize the exposed surfaces due to the porous nanofiber network and a plenty of hydrophilic groups along the cellulose chains. Second, the RGO sandwiched by PPY acts as a high conductive layer to ensure intimate contact and effective electron transport. Moreover, the PPY/RGO/BC flexible electrode enable the good electrochemical properties without sacrificing its mechanical performance.

Symmetric supercapacitors were assembled in two-electrode system containing two PPY₆/RGO/BC flexible electrodes separated by a cellulose acetate membrane immersed in 1 M Na₂NO₃ aqueous electrolyte. The CV of the symmetric device in flat and bending conditions was measured by demonstrating the toughness-enabled flexibility at the scan rate of 5 mV s⁻¹. The both plots show similar quasi-rectangular shapes without significant difference (Fig. 7a), indicating the highly flexible property for the PPY₆/RGO/BC based symmetrical supercapacitor. CV curves collected for the symmetric device can be operated under various scan rates up to 50 mV s⁻¹, indicating a good capacitive behavior (Fig. 7b). The GCD curves of the device at different current densities are collected in Fig. 7c,

which show nearly symmetry with linear slopes, implying a good reversibility for the device during the charge-discharge process. The calculated areal capacitance from GCD curves is 790 at a current density of 1 mA cm⁻², and still retain 360 at 30 mA cm⁻². It's worth noting that the bend state exerts small effect on the capacitive behavior in low-current-density region with a 2.8% decrease, but a 9.2% decrease in the high-density region (Fig. 7d), which could be attributed to increased ion diffusion resistance under a high rate caused by compact structure at bending state [10]. The long-term cycling performance of the device was tested at 10 mA cm⁻² (Fig. 7e). After 3000 cycles, the capacitance retention remains 75.8% of the initial capacitance. Ragone plot of the PPY₆/RGO/BC symmetric supercapacitor describes the relation between the areal power density and energy density at different current densities, as shown in Fig. 7f. The maximum areal energy density of the device reaches 0.11 mWh cm⁻² in flat state and at a power density of 0.5 mW cm⁻², which is higher than that of the most of reported conductive polymer flexible symmetric supercapacitor, while it can be still maintained 0.05 mWh cm⁻² at a power density of

15 mW cm⁻². After bending, the device also remains 0.106 mWh cm⁻² at a power density of 0.5 mW cm⁻² and 0.045 mWh cm⁻² at a power density of 15 mW cm⁻² (see Table 1).

4. Conclusions

In summary, a flexible and freestanding PPY/RGO/BC electrode is designed and fabricated in a simple, low-cost and effective approach. Comparing with conventional strategy of direct electropolymerization or chemical polymerization onto film, the proposed method achieves several advantages in terms of large areal mass of 8.93 mg cm⁻², high areal capacitance (2100 mF cm⁻²) and high flexibility. Moreover, the assembled symmetric supercapacitor delivers as high as 790 mF cm⁻² of areal capacitance and 0.11 mWh cm⁻² of energy density. These advantages make this hybrid paper a promising electrode for application in flexible energy storage devices.

Acknowledgement

The authors gratefully acknowledge financial supports from the Chang Jiang Scholars Program (51073047) and National Natural Science Foundation of China (91016015).

References

- [1] J. Wang, X.H. Li, Y.L. Zi, S.H. Wang, Z.L. Li, L. Zheng, F. Yi, S.M. Li, Z.L. Wang, A flexible fiber-based supercapacitor-triboelectric-nanogenerator power system for wearable electronics, *Adv. Mater.* 27 (2015) 4830–4836.
- [2] C.Y. Foo, A. Sumbaja, D.J.H. Tan, J.X. Wang, P.S. Lee, Flexible and highly scalable V₂O₅-rGO electrodes in an organic electrolyte for supercapacitor devices, *Adv. Energy Mater.* 4 (2014) 1400236.
- [3] Q.L. Zhou, X.K. Ye, Z.Q. Wan, C.Y. Jia, A three-dimensional flexible supercapacitor with enhanced performance based on lightweight, conductive graphene-cotton fabric electrode, *J. Power Sources* 296 (2015) 186–196.
- [4] M. Liu, S. He, W. Fan, Y.E. Miao, T. Liu, Filter paper-derived carbon fiber/polyaniline composite paper for high energy storage applications, *Compos. Sci. Technol.* 101 (2014) 152–158.
- [5] F. Wang, H.J. Kim, S. Park, C.D. Kee, S.J. Kim, I.K. Oh, Bendable and flexible supercapacitor based on polypyrrole-coated bacterial cellulose core-shell composite network, *Compos. Sci. Technol.* 128 (2016) 33–40.
- [6] S.H. Li, D.K. Huang, B.Y. Zhang, X.B. Xu, M.K. Wang, G. Yang, Y. Shen, Flexible supercapacitors based on bacterial cellulose paper electrodes, *Adv. Energy Mater.* 4 (2014) 1301655.
- [7] M. Hassan, K.R. Reddy, E. Haque, S.N. Faisal, S. Ghasemi, A.I. Minett, V.G. Gomes, Hierarchical assembly of graphene/polyaniline nanostructures to synthesize free-standing supercapacitor electrode, *Compos. Sci. Technol.* 98 (2014) 1–8.
- [8] J. Zhi, W. Zhao, X.Y. Liu, A. Chen, Z.Q. Liu, F.Q. Huang, Highly conductive ordered mesoporous carbon based electrodes decorated by 3D graphene and 1D silver nanowire for flexible supercapacitor, *Adv. Funct. Mater.* 24 (2014) 2013–2019.
- [9] M.F. Shao, Z.H. Li, R.K. Zhang, F.Y. Ning, M. Wei, D.G. Evans, X. Duan, Hierarchical conducting polymer@ clay core-shell arrays for flexible all-solid-state supercapacitor devices, *Small* 11 (2015) 3530–3538.
- [10] Z.Y. Xiong, C.L. Liao, W.H. Han, X.G. Wang, Mechanically tough large-area hierarchical porous graphene films for high-performance flexible supercapacitor applications, *Adv. Mater.* 27 (2015) 4469–4475.
- [11] M. Ghidui, M.R. Lukatskaya, M.Q. Zhao, Y. Gogotsi, M.W. Barsoum, Conductive two-dimensional titanium carbide/clay/with high volumetric capacitance, *Nature* 516 (2014) 78–81.
- [12] S.H. Li, D.K. Huang, J.C. Yang, B.Y. Zhang, X.F. Zhang, G. Yang, M.K. Wang, Y. Shen, Freestanding bacterial cellulose–polypyrrole nanofibres paper electrodes for advanced energy storage devices, *Nano Energy* 9 (2014) 309–317.
- [13] P.K. Kalamate, R.A. Dar, S.S.P. Karna, A.K. Srivastava, High performance supercapacitor based on graphene-silver nanoparticles-polypyrrole nanocomposite coated on glassy carbon electrode, *J. Power Sources* 276 (2015) 262–270.
- [14] C.Z. Yuan, L. Yang, L.R. Hou, J.Y. Li, Y.X. Sun, X.G. Zhang, L.F. Shen, X.J. Lu, S.L. Xiong, X.W. Lou, Flexible hybrid paper made of monolayer Co₃O₄ microsphere arrays on rGO/CNTs and their application in electrochemical capacitors, *Adv. Funct. Mater.* 22 (2012) 2560–2566.
- [15] A. Sumbaja, C.Y. Foo, X. Wang, P.S. Lee, Large areal mass, flexible and freestanding reduced graphene oxide/manganese dioxide paper for asymmetric supercapacitor device, *Adv. Mater.* 25 (2013) 2809–2815.
- [16] T.Y. Liu, L.R. Finn, M.H. Yu, H.Y. Wang, T. Zhai, X.H. Lu, Y.X. Tong, Y. Li, Polyaniline and polypyrrole pseudocapacitor electrodes with excellent cycling stability, *Nano Lett.* 14 (2014) 2522–2527.
- [17] T. Qian, C.F. Yu, S.S. Wu, J. Shen, A facilely prepared polypyrrole–reduced graphene oxide composite with a crumpled surface for high performance supercapacitor electrodes, *J. Mater. Chem. A* 1 (2013) 6539–6542.
- [18] C.Y. Yang, J.L. Shen, C.Y. Wang, H.J. Fei, H. Bao, G.C. Wang, All-solid-state asymmetric supercapacitor based on reduced graphene oxide/carbon nanotube and carbon fiber paper/polypyrrole electrodes, *J. Mater. Chem. A* 2 (2014) 1458–1464.
- [19] L.Y. Yuan, B. Yao, B. Hu, K.F. Huo, W. Chen, J. Zhou, Polypyrrole-coated paper for flexible solid-state energy storage, *Energy Environ. Sci.* 6 (2013) 470–476.
- [20] L.N. Ma, P. Zhao, W.J. Wu, H.J. Niu, J.W. Cai, Y.F. Lian, X.D. Bai, W. Wang, RGO functionalised with polyschiff base: multi-chemical sensor for TNT with acidochromic and electrochromic properties, *Polym. Chem.* 4 (2013) 4746–4754.
- [21] K. Liang, T.L. Gu, Z.Y. Cao, X.Z. Tang, W.C. Hu, B.Q. Wei, In situ synthesis of SWNTs @ MnO₂/polypyrrole hybrid film as binder-free supercapacitor electrode, *Nano Energy* 9 (2014) 245–251.
- [22] S. Bose, N.H. Kim, T. Kuila, K. Lau, J.H. Lee, Electrochemical performance of a graphene–polypyrrole nanocomposite as a supercapacitor electrode, *Nanotechnology* 22 (2011) 295202.
- [23] F. Zhang, F. Xiao, Z.H. Dong, W. Shi, Synthesis of polypyrrole wrapped graphene hydrogels composites as supercapacitor electrodes, *Electrochim. Acta* 114 (2013) 125–132.
- [24] J.B. Zhu, Y.L. Xu, J. Wang, J.P. Wang, Y. Bai, X.F. Du, Morphology controllable nano-sheet polypyrrole–graphene composites for high-rate supercapacitor, *Phys. Chem. Chem. Phys.* 17 (2015) 19885–19894.
- [25] H. Kashani, L.Y. Chen, Y. Ito, J.H. Han, A. Hirata, M.W. Chen, Bicontinuous nanotubular graphene–polypyrrole hybrid for high performance flexible supercapacitors, *Nano Energy* 19 (2016) 391–400.
- [26] J. Zhang, P. Chen, B.H.L. Oh, M.B.C. Park, High capacitive performance of flexible and binder-free graphene–polypyrrole composite membrane based on in situ reduction of graphene oxide and self-assembly, *Nanoscale* 5 (2013) 9860–9866.
- [27] Y. Shi, L.J. Pan, B.R. Liu, Y.Q. Wang, Y. Cui, Z.N. Bao, G.H. Yu, Nanostructured conductive polypyrrole hydrogels as high-performance, flexible supercapacitor electrodes, *J. Mater. Chem. A* 2 (2014) 6086–6091.
- [28] Y. Song, J.L. Xu, X.X. Liu, Electrochemical anchoring of dual doping polypyrrole on graphene sheets partially exfoliated from graphite foil for high-performance supercapacitor electrode, *J. Power Sources* 249 (2014) 48–58.
- [29] J. Zhang, X.S. Zhao, Conducting polymers directly coated on reduced graphene oxide sheets as high-performance supercapacitor electrodes, *J. Phys. Chem. C* 116 (2012) 5420–5426.
- [30] X.B. Zang, X. Li, M. Zhu, X.M. Li, Z. Zhen, Y.J. He, K.L. Wang, J.Q. Wei, F.Y. Kang, H.W. Zhu, Graphene/polyaniline woven fabric composite films as flexible supercapacitor electrodes, *Nanoscale* 7 (2015) 7318–7322.
- [31] L. Yuan, X. Xiao, T. Ding, J. Zhong, X. Zhang, Y. Shen, B. Hu, Y. Huang, J. Zhou, Z. Wang, Paper-based supercapacitors for self-powered nanosystems, *Angew. Chem. Int. Ed.* 51 (2012) 4934–4938.
- [32] F.H. Meng, Y. Ding, Sub-micrometer-thick all-solid-state supercapacitors with high power and energy densities, *Adv. Mater.* 23 (2011) 4098–4102.
- [33] K.W. Shu, C.Y. Wang, C. Zhao, Y. Ge, G.G. Wallace, A free-standing graphene-polypyrrole hybrid Paper via electropolymerization with an enhanced areal capacitance, *Electrochim. Acta* 212 (2016) 561–571.
- [34] C. Yang, L.L. Zhang, N.T. Hu, Z. Yang, H. Wei, Y.F. Zhang, Reduced graphene oxide/polypyrrole nanotube papers for flexible all-solid-state supercapacitors with excellent rate capability and high energy density, *J. Power Sources* 302 (2016) 39–45.
- [35] C.J. Raj, B.C. Kim, W.J. Cho, W. Lee, S.D. Jung, Y.H. Kim, S.Y. Park, K.H. Yu, Highly flexible and planar supercapacitors using graphite flakes/polypyrrole in polymer lapping film, *ACS Appl. Mater. Interfaces* 7 (2015) 13405–13414.
- [36] L.Y. Yuan, B. Yao, B. Hu, K.F. Huo, W. Chen, J. Zhou, Polypyrrole-coated paper for flexible solid-state energy storage, *Energy Environ. Sci.* 6 (2013) 470–476.